

# 1 **A bioorthogonal chemical reporter for fatty acid synthase-dependent protein acylation**

2

3 **Krithika P. Karthigeyan<sup>1</sup>, Lizhi Zhang<sup>2</sup>, David R. Loiselle<sup>3</sup>, Timothy A. J. Haystead<sup>3</sup>,**  
4 **Menakshi Bhat<sup>1</sup>, Jacob S. Yount<sup>2\*</sup>, Jesse J. Kwiek<sup>1\*</sup>**

5 1. Department of Microbiology and Center for Retrovirus Research, The Ohio State  
6 University, Columbus, Ohio, USA.

7 2. Department of Microbial Infection and Immunity, The Ohio State University, Columbus,  
8 Ohio, USA.

9 3. Department of Pharmacology and Cancer Biology, Duke University School of Medicine,  
10 Durham, NC, USA.

11 \*Co-corresponding authors. [Kwiek.2@osu.edu](mailto:Kwiek.2@osu.edu), [Jacob.Yount@osumc.edu](mailto:Jacob.Yount@osumc.edu)

12

## 13 **Summary**

14 Cells acquire fatty acids from dietary sources or via *de novo* palmitate production by fatty acid  
15 synthase (FASN). Although most cells express FASN at low levels, it is upregulated in cancers  
16 and during replication of many viruses. The precise role of FASN in disease pathogenesis is  
17 poorly understood, and whether *de novo* fatty acid synthesis contributes to host or viral protein  
18 acylation has been traditionally difficult to study. We describe a cell permeable, click-chemistry  
19 compatible alkynyl-acetate analog (Alk-4) that functions as a reporter of FASN-  
20 dependent protein acylation. In a FASN-dependent manner, Alk-4 selectively labeled the  
21 cellular protein interferon-induced transmembrane protein 3 (IFITM3) at its palmitoylation sites,  
22 and the HIV-1 matrix protein at its myristoylation site. Alk-4 metabolic labeling also enabled  
23 biotin-based purification and identification of more than 200 FASN-dependent acylated cellular  
24 proteins. Thus, Alk-4 is a useful bioorthogonal tool to selectively probe FASN-mediated protein  
25 acylation in normal and diseased states.

26

27

28 **Keywords:** fatty acid synthase, click chemistry, S-palmitoylation, N-myristoylation, HIV-1,

29 Influenza, fatty acylation, IFITM3, HIV-1 Gag, CD9.

## 30 **Introduction**

31 Long chain fatty acids (FA) are essential components of lipid bilayers, are used to store energy  
32 liberated by  $\beta$ -oxidation, and are covalently attached to proteins to increase hydrophobicity and  
33 regulate subcellular localization.<sup>1</sup> Long chain fatty acids can be obtained exogenously through  
34 dietary sources, or endogenously via *de novo* fatty acid biosynthesis.<sup>2</sup> Mammalian fatty acid  
35 synthase (FASN) is a 272 kDa cytosolic enzyme that catalyzes the complete *de novo*

36 synthesis of palmitate from acetyl-CoA and malonyl-CoA. The final product, palmitic acid (16:0)  
37 is then released from FASN, where it can be metabolized by  $\beta$ -oxidation into myristic acid  
38 (14:0), or other long chain FA.<sup>3</sup> FASN expression is highly regulated in cells and its expression  
39 can change dramatically in response to stresses such as starvation, lactation or pathological  
40 states.<sup>3</sup> Increased *de novo* FA biosynthesis and FASN up-regulation have been observed in  
41 breast cancer, melanoma, and hepatocellular carcinoma.<sup>4</sup> Studies of enveloped viruses  
42 including hepatitis B virus,<sup>5</sup> Dengue virus,<sup>6</sup> Epstein-Barr virus,<sup>7</sup> hepatitis C virus,<sup>8</sup> HIV-1,<sup>9</sup>  
43 Chikungunya virus,<sup>10,11</sup> and West Nile virus<sup>12,13</sup> indicate that many viruses both upregulate and  
44 require host FASN activity for effective replication. The contributions of *de novo* synthesized  
45 FA to post-translational modifications of viral and host proteins remains understudied.

46 Identification of protein acylation has been challenging due to the lack of antibodies  
47 against lipid modifications, and inefficiencies of standard mass spectrometry techniques to  
48 identify acylated proteins.<sup>14</sup> While protein myristoylation site prediction is facilitated by a  
49 consensus sequence motif on nearly all myristoylated proteins (Met-Gly-XXX-Ser/Thr),<sup>1</sup> protein  
50 palmitoylation site prediction remains challenging due to the lack of a consensus sequence.<sup>15</sup>  
51 To measure acyl-group synthesis mediated by FASN and the fate of the *de novo* synthesized  
52 fatty acids, one must use <sup>14</sup>C labeled acetate, which suffers from low detection sensitivity,  
53 general complications associated with radioisotope work,<sup>16</sup> and an inability to selectively enrich  
54 acylated proteins. Over the last decade, bioorthogonal labeling and detection of protein fatty  
55 acylation using click chemistry compatible analogs of palmitate and myristate have provided  
56 quick and sensitive methods for detection of protein acylations.<sup>17,18</sup> The copper-catalyzed  
57 azide-alkyne cycloaddition (CuAAC) reactions enable labeling of cells with alkynyl analogs of  
58 fatty acids that can be reacted with azides conjugated to suitable detection tags, such as  
59 fluorophores, or affinity tags, including biotin.<sup>19,20</sup> Although very useful, palmitate and myristate  
60 analogs only measure the acylation state of proteins modified by the exogenous chemical

61 reporters. Given the critical role of FASN-dependent *de novo* synthesized fatty acids in cancer,  
62 metabolic disorders, and viral replication, we posit that a bioorthogonal reporter of FASN-  
63 dependent protein acylation will facilitate a better understanding of the contributions of FASN-  
64 dependent protein fatty acylation to protein function, protein localization, and FASN-mediated  
65 pathogenesis. Here we demonstrate the utility of 5-hexynoic acid, or Alk-4, a cell permeable,  
66 click-chemistry compound that labels proteins acylated by products of FASN-mediated *de novo*  
67 fatty acid biosynthesis.

68

## 69 **Results**

70 **Alk-4 labels palmitoylated proteins at known palmitoylation sites.** Bioorthogonal reporters  
71 such as alkynyl palmitate (“Alk-16”) and alkynyl myristate (“Alk-12”) are substrates of  
72 palmitoyltransferase and myristoyltransferase activity that are often used to identify  
73 palmitoylated and myristoylated proteins.<sup>21–23</sup> Because these reporters mimic the end product  
74 of FASN activity (palmitate) or palmitate oxidation (myristate), Alk-12 and Alk-16 cannot be  
75 used to determine the source of the fatty acyl adduct (i.e. exogenous/imported or  
76 endogenous/*de novo* synthesized). We hypothesized that a cell permeable, bioorthogonal  
77 mimic of a putative FASN substrate, 5-hexynoate (termed Alk-4 here)<sup>24</sup> could be used to study  
78 the contributions of FASN-mediated *de novo* fatty acid synthesis to protein acylation (Figure  
79 1a,b). To determine whether Alk-4 selectively labels palmitoylated proteins, we tested whether  
80 a known palmitoylated protein, IFITM3, was labeled upon a 24 hour treatment of cells with  
81 alkynyl acetate analogues of different carbon chain lengths, Alk-3 and Alk-4, in comparison  
82 with the well-established palmitoylation reporter Alk-16 (Figure 1a, b). Alk-16 robustly labeled  
83 IFITM3 as detected by click-chemistry tagging of immunoprecipitated IFITM3 with azido-  
84 rhodamine and fluorescence gel scanning. Alk-4 also successfully labeled IFITM3, while Alk-3

85 showed minimal labeling (Figure 2a). Next, we tested whether Alk-4 labeling of IFITM3  
86 occurred on its known palmitoylated cysteines.<sup>22</sup> A triple cysteine to alanine palmitoylation-  
87 deficient mutant of IFITM3 (termed Palm $\Delta$ ), was not labeled by either Alk-16 or Alk-4 (Figure  
88 2b). To further test the ability of Alk-4 to label palmitoylated proteins, we examined whether the  
89 tetraspanin CD9, which has 6 palmitoylated cysteines, was also labeled by Alk-4. Similar to  
90 IFITM3, CD9 was labeled by Alk-4, while a mutant CD9 in which its palmitoylated cysteines  
91 were mutated to alanine (termed CD9-Palm $\Delta$ ), was not labeled (Figure 2c). These results  
92 indicate that Alk-4 is metabolized into a click-chemistry functionalized fatty acid adduct that is  
93 specifically incorporated onto protein palmitoylation sites.

94 **Alk-4 metabolism provides a substrate used by DHHC palmitoyltransferases.** Many  
95 proteins are reversibly palmitoylated at cysteine residues<sup>25</sup> by aspartate-histidine-histidine-  
96 cysteine (DHHC) palmitoyltransferases. DHHC palmitoyltransferases primarily use palmitoyl-  
97 CoA (C16:0) to modify cysteine residues on proteins, although DHHC's can tolerate substrates  
98 with carbon chain lengths as short as 14 and as long as 20.<sup>26,27</sup> Acyl chains with fewer than 14  
99 carbons have not been detected on cysteines, indicating that DHHC enzymes disfavor short  
100 chain fatty acids as substrates.<sup>28-31</sup> Given the selectivity of the DHHC palmitoyltransferases for  
101 long chain fatty acids, we sought to determine whether labeling of IFITM3 by Alk-4 was  
102 affected by DHHC7 overexpression, which was previously shown to be among the enzymes  
103 that can catalyze IFITM3 palmitoylation.<sup>32</sup> In cells incubated with Alk-4, DHHC7  
104 overexpression increased IFITM3 labeling, while overexpression of a dominant negative  
105 DHHC7 mutant decreased IFITM3 labeling (Figure 2d). These results indicate that Alk-4 is  
106 metabolized into a long chain fatty acid that can be used as a substrate by DHHC  
107 palmitoyltransferases for protein palmitoylation.



108 **Labeling of IFITM3 by Alk-4 requires FASN.** We have previously shown that IFITM3  
109 palmitoylation is required for its antiviral activity against influenza virus infection.<sup>22,33</sup> To  
110 determine if FASN-mediated *de novo* fatty acid biosynthesis contributes to an IFN $\beta$ -regulated  
111 IFITM3-mediated antiviral response, we measured endogenous IFITM3 labeling by Alk-4 in  
112 wild-type (WT) and FASN knockout HAP1 cells. As expected, IFN $\beta$  induced endogenous  
113 IFITM3 expression, and IFITM3 upregulation was independent of FASN expression (Figure  
114 2e). In WT cells, Alk-4 treatment resulted in robust endogenous IFITM3 labeling that was  
115 absent in FASN-deficient cells (Figure 2f). Thus, we show for the first time that FASN  
116 contributes to the palmitoylation of endogenous IFITM3. Owing to the observations that IFITM3  
117 is required for an effective IFN $\beta$ -mediated anti-influenza response,<sup>32</sup> that palmitoylation of  
118 IFITM3 is required for its antiviral activity<sup>32</sup>, and that FASN regulates Alk-4 mediated IFITM3  
119 palmitoylation (Figure 2f), we sought to determine the effect of FASN expression on IFN $\beta$ -  
120 mediated inhibition of influenza virus infection. In the absence of IFN $\beta$ , FASN expression had  
121 no effect on influenza infection (Figure 2g). However, IFN $\beta$ -mediated inhibition of influenza  
122 virus infection was significantly decreased in the absence of FASN expression (Figure 2g),  
123 suggesting that FASN-dependent palmitate synthesis likely contributes to the palmitoylation-  
124 dependent antiviral activity of IFITM3.

125 **Alk-4 labeling of myristoylated proteins is FASN dependent.** Acetyl CoA is condensed with  
126 malonyl-CoA and elongated by FASN to generate palmitate for protein palmitoylation. To  
127 generate myristoyl CoA for myristoylation, palmitoyl CoA must be  $\beta$ -oxidized to myristoyl CoA  
128 before it is covalently attached to glycine residues by N-myristoyl transferases (Figure 4d).<sup>34,1</sup>  
129 To determine if Alk-4 is metabolized into a fatty acid analog that can selectively label  
130 myristoylated proteins, we tested whether a known myristoylated protein, HIV-1 matrix protein  
131 (MA), was labeled upon a 24-hour incubation with Alk-4. HEK293T cells were transfected with  
132 flag-tagged HIV-1 MA, or the myristoylation deficient matrix-G2A mutant (MA-G2A) and treated

133 with Alk-4 or Alk-12 (an established chemical reporter of myristoylation). Immunoprecipitation  
134 of flag-tagged matrix and subsequent click reaction with azido-rhodamine revealed labeling of  
135 HIV-1 matrix in cells incubated with Alk-4 or Alk-12 (Figure 3a). The G2A-MA Gag protein,  
136 which cannot be myristoylated, was not labeled by Alk-4, indicating myristoylation site-specific  
137 labeling of HIV-1 matrix protein by Alk-4. Treatment of cells with Fasnall,<sup>9,35</sup> a FASN inhibitor,  
138 abolished Alk-4 labeling of HIV-1 matrix protein. As a control, Fasnall treatment did not disrupt  
139 HIV-1 matrix protein labeling by Alk-12. To confirm the selective labeling of HIV-1 matrix  
140 protein that we observed with fluorescence-based click reactions, cell lysates were instead  
141 reacted with biotin azide. Biotin-conjugated proteins were precipitated with streptavidin  
142 agarose and bound proteins were released with sodium dithionite, which cleaves a diazo linker  
143 within the azido-biotin molecule, enabling selective elution of Alk-4 labeled proteins. Eluents  
144 were probed for the MA-Flag proteins, and, in the presence of Alk-4, HIV-1 matrix protein was  
145 recovered. HIV-1 matrix protein recovery was diminished both when a myristoylation deficient  
146 HIV-1 matrix protein variant was transfected (MA-G2A) (Figure 3b) and when FASN was  
147 inhibited by Fasnall. These results indicate that Alk-4 is metabolized into a fatty acid adduct  
148 that is specifically incorporated onto protein myristoylation sites in a FASN-dependent manner,  
149 and that can be detected by multiple labeling modalities.

150 **FASN-dependent, Alk-4 mediated metabolic labeling of endogenous fatty acylated**  
151 **proteins.** To test the utility of Alk-4 as a global indicator of FASN-dependent protein acylation,  
152 we incubated the human fibroblast-like cell line HAP1 or a FASN-deficient clone of the HAP1  
153 cells with Alk-4 or a vehicle control (DMSO). Following metabolic labeling of HAP1 cells with  
154 Alk-4, cell lysates were reacted with azido-biotin and labeled proteins were precipitated as  
155 described in Figure 3b. Eluents were then probed for proteins known to be palmitoylated  
156 (Calnexin)<sup>36</sup> or myristoylated (Src).<sup>37,38</sup> In wild-type HAP1 cells, Alk-4 labeling recovered both  
157 Calnexin and Src, while in FASN-deficient cells, incubation with Alk-4 did not enable Calnexin

158 or Src recovery (Figure 4a). To determine the breadth of proteins recovered from cells  
159 incubated with Alk-4, we next used mass spectrometry to identify biotinylated proteins from  
160 HAP1 cells with or without Alk-4 and with or without FASN. FASN was only recovered from WT  
161 HAP1 cells incubated with Alk-4, consistent with the acyl intermediates formed between FASN  
162 and the elongating fatty acid chain (Figure 4d).<sup>39</sup> This experiment also recovered, in an Alk-4  
163 dependent manner, several enzymes involved in the metabolism of acetate to palmitate and  
164 myristate, including acetyl CoA synthetase (ACSA), acetyl CoA carboxylase 1 (ACACA), and  
165 multiple enzymes involved in fatty acid beta-oxidation (Figure 4d, Supplementary table 2). In  
166 total, Alk-4 labeling enabled recovery of 264 proteins in an Alk-4 and FASN-dependent manner  
167 (Figure 4b). Of these, 77% (203) have previously been identified in at least one palmitoyl  
168 proteome or they have been experimentally validated to be palmitoylated. These included well  
169 characterized palmitoylation substrates, such as Guanine nucleotide-binding protein G  
170 (GNAI1) and Catenin beta-1 (CTNB1) (Figure 4c, Supplementary table 1 & 3). Of the  
171 remaining proteins that were purified, 17% were predicted to be palmitoylated (e.g. SAM  
172 domain and HD domain-containing protein 1 [SAMHD1]), and 3% were predicted to be  
173 myristoylated (e.g. ribosomal protein S6 kinase alpha [KS6A1])<sup>40,41</sup> (Figure 4c, Supplementary  
174 Table 1 & 4).

175

## 176 **Discussion**

177 We describe a click-chemistry compatible FASN-substrate, Alk-4 (5-hexynoate), which  
178 selectively labels both palmitoylated (*e.g.* IFITM3, CD9) and myristoylated (*e.g.* HIV-1 matrix)  
179 proteins. Click chemistry compatible substrate analogs like Alk-4 overcome several inherent  
180 disadvantages of radiolabeling, such as long sample processing and film exposure times with  
181 low sensitivity.<sup>16</sup> Moreover, click chemistry reactions can be combined with several detection

182 methods that are compatible with high throughput applications including mass spectrometry-  
183 based proteomics, flow cytometry, fluorescence microscopy, and live cell imaging.<sup>21</sup> Beyond  
184 identification of FASN-dependent protein acylation, Alk-4 has more functionality than a  
185 radiolabeled FASN substrate because it can be reacted with azido-biotin to facilitate  
186 streptavidin-based purification of FASN-dependent acylated proteins. We are not the first to  
187 suggest the utility of Alk-4, which has previously been evaluated as a chemical tool to monitor  
188 protein acetylation at shorter timescales, although it was noted that some of the acetylation  
189 reporters were incorporated onto proteins by chemical acylation.<sup>24</sup> Nevertheless, our finding  
190 that FASN activity is required for Alk-4 labeling of multiple proteins such as IFITM3, HIV-1  
191 matrix, Calnexin, and Src strongly supports the use of Alk-4 as a selective reporter of FASN-  
192 dependent protein acylation.

193 FASN activity is required for replication of several enveloped viruses, including  
194 Chikungunya,<sup>10</sup> HIV-1,<sup>9</sup> Influenza,<sup>42</sup> and SARS-CoV-2,<sup>43</sup> and many others.<sup>6,7,13</sup> FASN inhibitors,  
195 including Fasnall<sup>9,35</sup> and the TVB compounds<sup>44,45</sup> have therapeutic potential, and  
196 pharmacological inhibition of FASN has been shown to modulate fatty acylation of viral proteins,  
197 including Chikungunya virus nsP1 palmitoylation,<sup>46</sup> SARS-CoV-2 spike palmitoylation,<sup>43</sup> and  
198 HIV-1 Gag myristoylation (Figure 3). In other cases, modulation of FASN activity affects host  
199 proteins that regulate infection, including MYD88 palmitoylation,<sup>47</sup> and the results presented  
200 here that reveal that FASN activity is required for an effective IFN $\beta$  immune response against  
201 influenza virus, possibly by providing fatty acyl moieties for modification of IFITM3. Increased *de*  
202 *novo* FA biosynthesis and FASN up-regulation has also been observed in breast cancer,  
203 melanoma, and hepatocellular carcinoma<sup>4</sup>, and *de novo* fatty acid biosynthesis and lipogenesis  
204 has been shown to be essential for protein palmitoylation of Ras, Wnt<sup>48</sup>, Calnexin<sup>49</sup>, and Src<sup>50</sup>  
205 in proliferating cells.<sup>51,52</sup> In tumor cells, FASN inhibition can have consequences beyond

206 inhibition of protein acylation<sup>53</sup>; *de novo* fatty acid biosynthesis has also been shown to be  
207 essential for membrane remodeling in tumor cells, where palmitate depletion via FASN inhibition  
208 led to disruption of lipid rafts and signaling pathways, ultimately resulting in apoptosis of tumor  
209 cells.<sup>54</sup> Thus, *de novo* fatty acid biosynthesis is a broadly utilized, fundamental metabolic  
210 pathway exploited during carcinogenesis and virus replication, and Alk-4 and its ability to  
211 measure flux through the *de novo* FASN pathway provides a new tool to better understand the  
212 role of FASN-dependent protein acylation during FASN-dependent pathologies.

213

## 214 **METHODS**

215 **Reagents, transfections, and infections.** Reagents, including 5-hexynoic acid (Alk-4), were  
216 purchased from Sigma (St. Louis, MO) or Thermo Fisher Scientific, unless stated otherwise.  
217 Alk-12 and Alk-16 were synthesized by the Hang lab according to published protocols.<sup>21</sup> Alk  
218 compounds were diluted in dimethyl sulfoxide (DMSO). HEK 293Ts were obtained from the  
219 American Type Culture Collection and were maintained in DMEM supplemented with 10%  
220 heat-inactivated fetal bovine serum (FBS; Serum Source International, Charlotte, NC) and 1%  
221 Penicillin/Streptomycin. HAP1 wild-type and HAP-1 FASN knockout cells were obtained from  
222 Horizon Discovery (Lafayette, Colorado) and were maintained in IMDM supplemented with  
223 10% heat-inactivated FBS and 1% Penicillin/Streptomycin. HIV-1 matrix plasmids pQCXIP-  
224 MA-FH (pMA-Flag) and pQCXIP-G2A-FH (pG2A-MA-Flag) were kindly provided by Dr.  
225 Stephen Goff, Columbia University.<sup>55</sup> HA-tagged IFITM3<sup>22</sup> and HA-tagged ZDHHC7<sup>56</sup> have  
226 been described. Cells were transfected using Genefect (Alkali Scientific, Fort Lauderdale, FL)  
227 or LipoJet transfection reagents (Signagen Laboratories, Rockville, MD), according to each  
228 manufacturer's protocol. Fasnall was synthesized as described.<sup>35</sup> Influenza virus H1N1 strain  
229 PR8 was propagated in 10-day-old embryonated chicken eggs (Charles River) for 48 hours at  
230 37 °C as described previously.<sup>57,58</sup> IFN $\beta$ -treated HAP1 WT and FASN KO cells were treated

231 with IFN overnight or left untreated as described previously<sup>32</sup>, and infected with H1N1 for 24  
232 hours (MOI = 1). Cells were stained with anti-influenza virus nucleoprotein antibodies to  
233 measure percentage of infection by flow cytometry.

234 **Metabolic labeling, immunoprecipitations, and CuAAC:** Cells were incubated for 24 hours  
235 with the indicated concentrations of Alk-3, Alk-4, Alk-12, Alk-16, or 0.001% DMSO in media  
236 supplemented with 1% charcoal-stripped FBS (Serum Source International, Catalog number  
237 FB02- 500CS), and then collected and washed thrice in ice-cold 1x phosphate buffered saline  
238 (PBS). Cells were lysed for 10 minutes on ice in 100 $\mu$ l 1% Brij buffer (1% (w/v) Brij O10,  
239 150mM NaCl, 50 mM triethanolamine with 1x EDTA-free complete protease inhibitor cocktail.  
240 Protein concentration was determined using the BCA assay. Flag precipitations used 500  $\mu$ g of  
241 cell lysate mixed with Protein G coated agarose beads and incubated with Anti-Flag antibody  
242 (catalog number F3165) for 2 hours at 4°C. Anti-HA IPs were performed using EZview Red  
243 Anti-HA Affinity Gel. Protein-conjugated beads were washed thrice with  
244 radioimmunoprecipitation assay (RIPA) buffer (50 mM triethanolamine, 150 mM NaCl, 1%  
245 sodium deoxycholate, 1% triton-X-100, 0.1 % SDS). Protein complexes bound to antibody  
246 coated beads were released by adding 4% SDS buffer (150 mM NaCl, 50 mM triethanolamine,  
247 4% [w/v] SDS), and the click reaction was initiation by addition of 2.75 $\mu$ l of click chemistry  
248 master mix (0.5 $\mu$ l of 5mM azido-rhodamine or tetramethylrhodamine-5-carbonyl azide [Click  
249 Chemistry Tools, Scottsdale, AZ ] in DMSO, 0.5 $\mu$ l of 50mM tris(2-carboxyethyl)phosphine  
250 [TCEP], 0.5 $\mu$ l of 50mM CuSO<sub>4</sub>, and 1.5 $\mu$ l of 2mM tris (1-benzyl-1H-1,2,3-triazol-4-  
251 yl)methyl)amine (TBTA) in 1:4 [v/v] DMSO/butanol). Reactions were incubated for one hour at  
252 room temperature, and proteins were eluted from the beads by heating at 95°C for 5 minutes  
253 in 4X SDS sample loading buffer (40% (v/v) glycerol, 240 mM Tris·Cl, pH 6.8, 8% (w/v) sodium  
254 dodecyl sulfate (SDS), 0.04% (w/v) bromophenol blue, 5% 2-mercaptoethanol). Eluted proteins

255 were resolved on 4-20% tris-glycine gels. To detect fluorescently labeled proteins, the gel was  
256 destained in 40% distilled water(v/v), 50%(v/v) methanol, 10%(v/v) acetic acid and visualized  
257 using on an Amersham Typhoon 9410 with 532-nm excitation and 580-nm detection filters. For  
258 biotin-based click reactions, Alk-4 incubated cells were lysed with 50 $\mu$ l 4% SDS buffer with 1x  
259 EDTA-free protease inhibitors supplemented with benzonase nuclease (Catalog number  
260 E1014). One mg of cell lysate was resuspended in 445 $\mu$ l 1x SDS buffer with 1x EDTA-free  
261 protease inhibitors and incubated for 1.5 hours with 55 $\mu$ l of click reaction master-mix consisting  
262 of 10 $\mu$ l of 5mM diazo biotin azide (Click Chemistry Tools), 10 $\mu$ l of 50mM TCEP, 25 ul of 2mM  
263 TBTA, 10 $\mu$ l of 50mM CuSO<sub>4</sub>. Proteins were precipitated using chloroform-methanol to remove  
264 unreacted biotin azide, and the precipitant was resuspended in 100 $\mu$ l 4% SDS buffer  
265 containing protease inhibitors supplemented and 2 $\mu$ l of 0.5M EDTA solution to chelate residual  
266 copper. Equivalent amount of protein in 100 $\mu$ l 4%SDS buffer and 200  $\mu$ l 1% Brij buffer with  
267 EDTA-free protease inhibitors was incubated with 75ul streptavidin agarose (EMD Millipore) for  
268 two hours at room temperature. Protein-conjugated beads were washed once in PBS/0.2-1%  
269 SDS, and thrice in PBS. Labeled proteins were selectively eluted by two elutions with 50mM  
270 sodium dithionite, desalted using spin desalting columns, mixed with 4X SDS sample loading  
271 buffer, and resolved on 10-12% Tris-Glycine gel. Coomassie staining was done using standard  
272 techniques.<sup>59</sup>

273 **Western blotting:** Proteins were transferred onto PVDF membrane (Bio-Rad, Hercules, CA),  
274 blocked with 5% bovine serum albumin dissolved in 1x tris-buffered saline (TBS) containing  
275 0.1% Tween-20. Anti-Flag (catalog number F3165) and Anti-FASN (catalog number  
276 SAB4300700) antibodies were purchased from Sigma and used at a final concentration of  
277 1:1000; anti-Calnexin (catalog number 2679S) and anti-Src (catalog number 2109S) antibodies  
278 were purchased from Cell Signaling Technologies (Danvers, MA) and used at a final



279 concentration of 1:2000. Anti-rabbit secondary antibody (Thermo Fisher Scientific catalog  
280 number 31460) was used at a final concentration of 1: 5000, and anti-mouse secondary  
281 antibody (Cell Signaling Technology catalog number 7076S) was used at a final concentration  
282 of 1:2000.

283 **Protein identification:** Capillary-LC-MS/MS was performed using a Thermo Scientific orbitrap  
284 fusion mass spectrometer equipped with an EASY-Spray™ Sources operated in positive ion  
285 mode. Samples were separated on an easy spray nano column (Pepmap™ RSLC, C18 3μ  
286 100A, 75μm X150mm Thermo Scientific) using a 2D RSLC HPLC system from Thermo  
287 Scientific. The full scan was performed at FT mode and the resolution was set at 120,000.  
288 EASY-IC was used for internal mass calibration. Mass spectra were searched using Mascot  
289 Daemon by Matrix Science version 2.3.2 (Boston, MA) and the database searched  
290 against Uniprot Human database (version 12032015). Data from two independent experiments  
291 were compiled on Scaffold Visualization software (Scaffold 4.9.0, Proteome Software Inc.,  
292 Portland, OR). Proteins were identified based on total spectrum count with a 1% false  
293 discovery rate (FDR) and a minimum of two peptides. Proteins were considered high  
294 confidence hits if they had DMSO spectral count of zero, and a minimum spectral count of five  
295 in both replicates. Putative fatty acylation sites in high confidence proteins were identified in  
296 the SwissPalm protein S-palmitoylation database (Version 3, <https://SwissPalm.org/>) using  
297 Dataset 3 (proteins found in at least one palmitoyl-proteome or experimentally validated to be  
298 palmitoylated) and Dataset 1 (All datasets). Protein sequences were also searched against  
299 GPS-Lipid using high threshold settings (Version 1.0, <http://lipid.biocuckoo.org/>), as described  
300 in the supplementary methods section.

301

302

### 303 **Acknowledgements**

304 This work was supported by NIH/NIAID grants AI141037 to J.J.K and AI130110 and AI142256  
305 to J.S.Y., and The Ohio State University Department of Microbiology. We thank Dr. Howard  
306 Hang of The Scripps Research Institute for providing Alk-12, Alk-16, and azido-rhodamine, and  
307 Dr. Yiping Zhu and Dr. Stephen Goff of Columbia University for providing MA-Flag and G2A-  
308 MA-Flag constructs. We thank Dr. Liwen Zhang of the OSU Mass spectrometry and  
309 Proteomics facility for acquisition and processing of the LC-MS/MS data under support from  
310 NIH Grants CA016058 and OD018056.

311

### 312 **Author Contributions**

313 K.P.K., J.S.Y., and J.J.K. conceived the project and wrote the paper. K.P.K. and L.Z.  
314 performed all experiments. K.P.K., L.Z., J.S.Y., and J.J.K. performed data analysis. M.B.,  
315 D.R.L., and T.A.J.H. provided experimental expertise. All authors edited and approved the  
316 manuscript.

317

### 318 **Competing Interests**

319 The authors declare no competing interests.

320

321

322

323

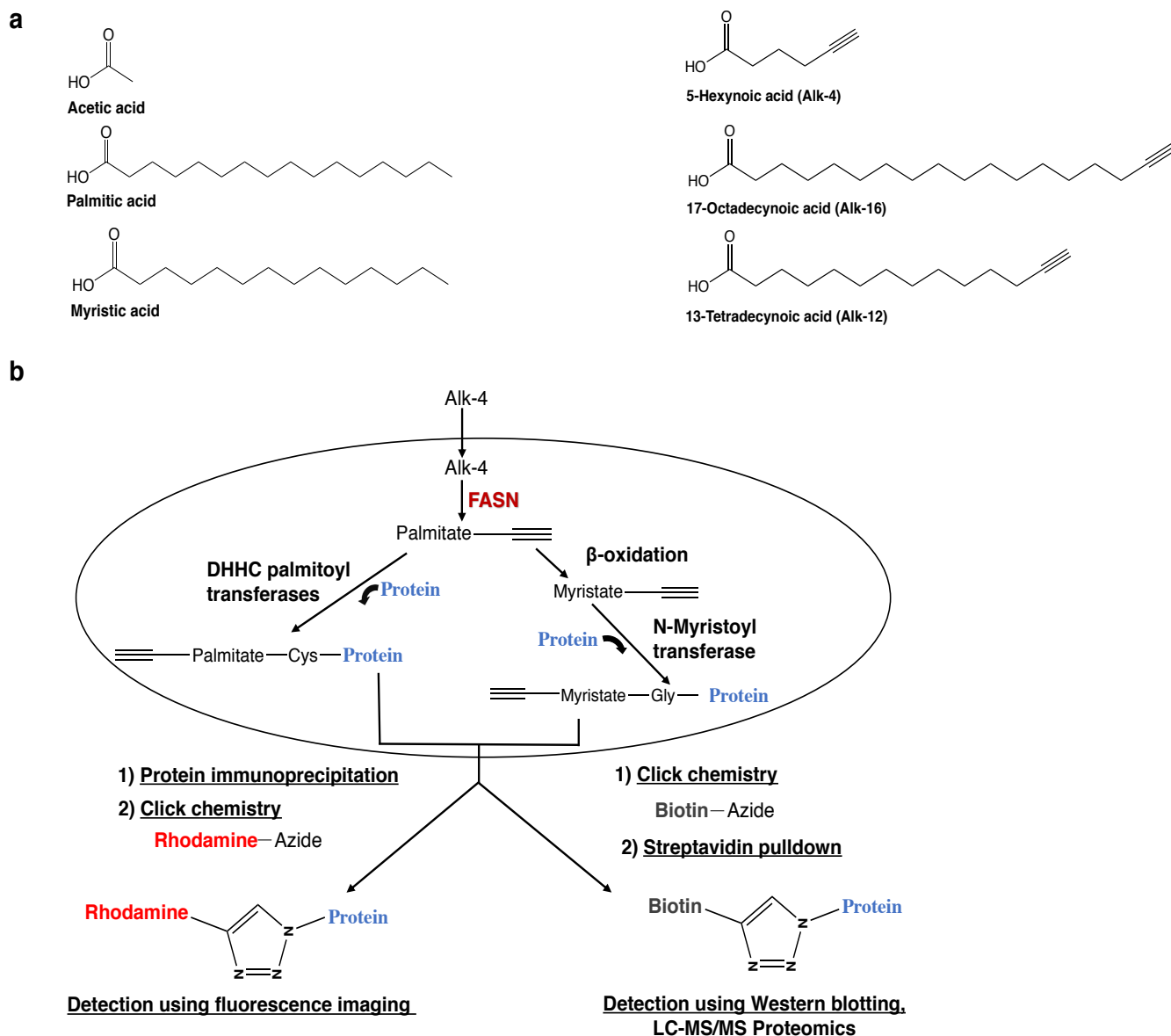
324

325

326

327

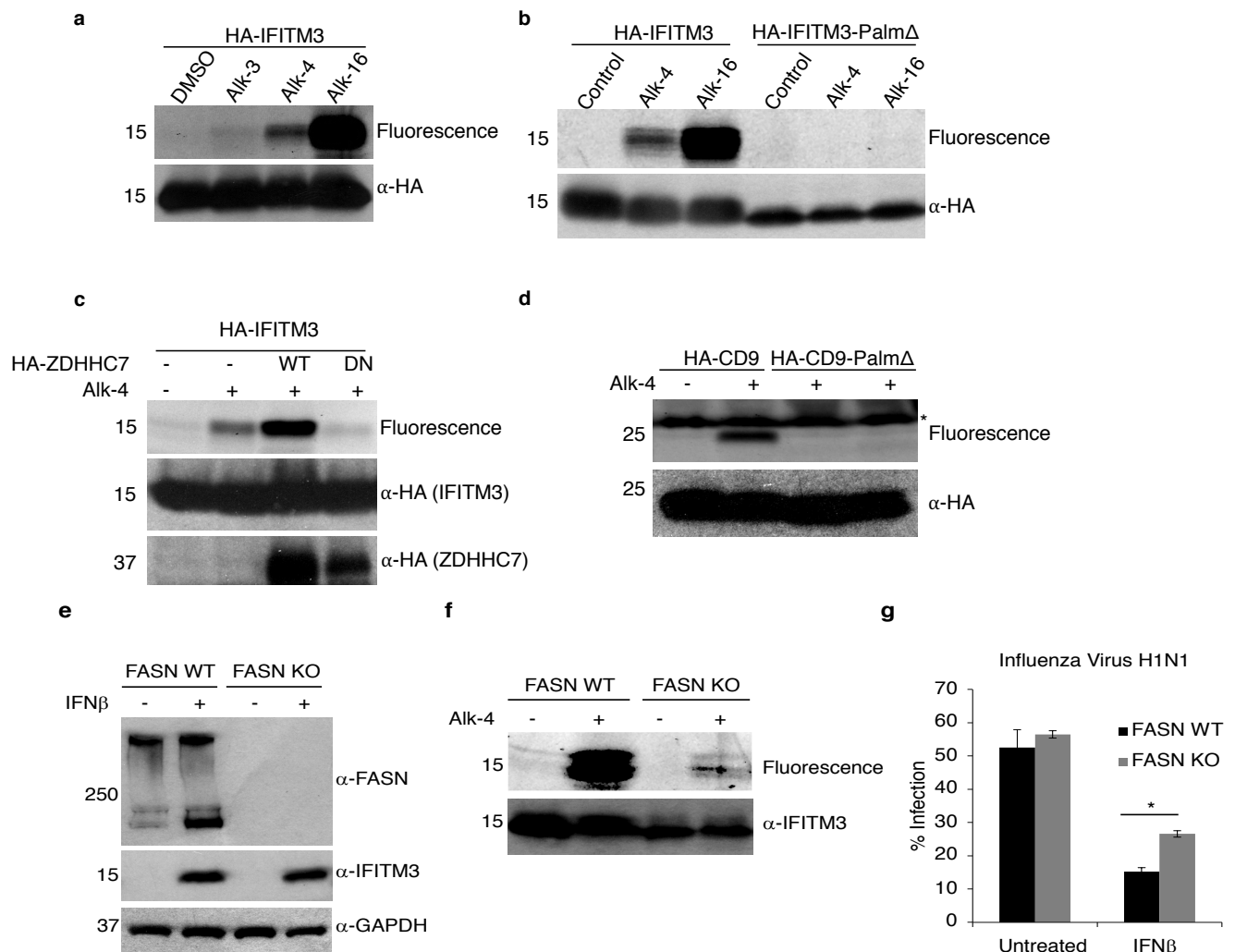
328 **Figures**



329

330 **Figure 1: Analog structures and schema depicting Alk-4 metabolism and incorporation**  
 331 **onto protein acylation sites. (a)** Structures of acetate, palmitate, and myristate, followed by  
 332 their click chemistry-compatible analogs Alk-4, Alk-16, and Alk-12. **(b)** 5-Hexynoic acid (Alk-4)  
 333 can be metabolized through the endogenous FASN pathway to yield functionalized versions of  
 334 fatty acyl groups that are transferred onto protein acylation sites by palmitoyl or N-myristoyl  
 335 transferases. Copper-catalyzed azide-alkyne cycloaddition (CuAAC) click reaction of proteins  
 336 containing the functionalized alkyne group to an azide-conjugated fluorophore such as  
 337 rhodamine can be used for fluorescence imaging, while CuAAC click reaction of alkyne-  
 338 containing proteins to an azide-conjugated biotin can be used for affinity purification and  
 339 subsequent western blotting or proteomics.

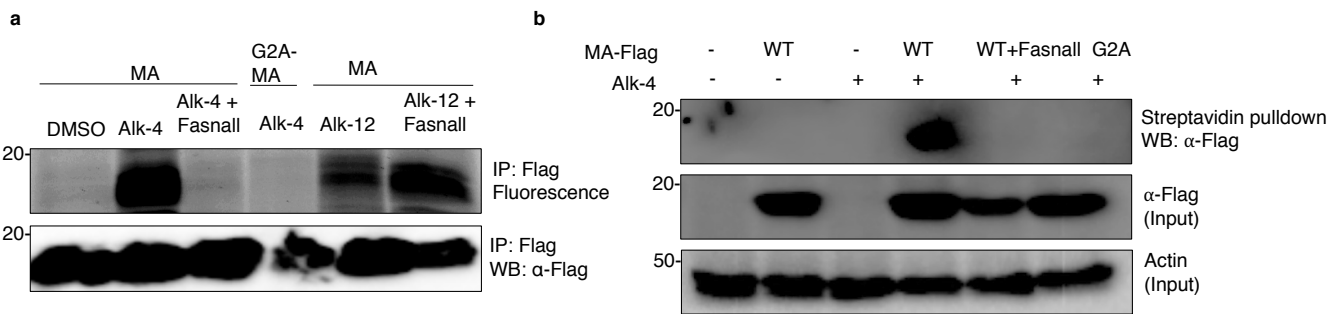
340



341

342 **Figure 2: FASN-dependent incorporation of Alk-4 at known protein palmitoylation sites**  
 343 **(a)** Immunoprecipitated HA-IFITM3 from HA-IFITM3 transfected 293Ts followed by rhodamine  
 344 azide click reaction revealed detectable labeling by Alk-16 and Alk-4 and minimal labeling by  
 345 Alk-3. **(b)** A triple cysteine to alanine IFITM3 mutant (Palm $\Delta$ ) was not labeled by Alk-4,  
 346 suggesting that Alk-4 labeling of IFITM3 occurred on known palmitoylated cysteines. **(c)** Alk-4  
 347 labeled CD9, while a mutant where its six palmitoylated cysteines were mutated to alanine was  
 348 not labeled, revealing that Alk-4 labels CD9 on known palmitoylated cysteines. **(d)** DHC  
 349 palmitoyltransferase overexpression increased Alk-4 labeling of IFITM3, while a dominant  
 350 negative mutant partially decreased labeling, suggesting that Alk-4 is metabolized into a long  
 351 chain fatty acid utilized by DHC palmitoyltransferases (\* indicates 25kDa fluorescent  
 352 molecular weight standard bleed through). **(e)** To test the requirement of FASN for labeling of  
 353 endogenous IFITM3 in cells treated with IFN $\beta$ , HAP1 WT and FASN KO cells were labeled  
 354 with Alk-4. Western blotting to confirm FASN levels in WT and KO cells, and expression of  
 355 endogenous IFITM3 on IFN $\beta$  treatment. **(f)** Alk-4 labeling of endogenous IFITM3 was only  
 356 observed in WT cells and not detected in FASN KO cells, indicating that FASN contributes to  
 357 palmitoylation of IFITM3. **(g)** IFN $\beta$  was significantly less effective at inhibiting Influenza virus  
 358 strain H1N1 infection in FASN KO cells (\* $p = 0.0002$ ), indicating that FASN is required for  
 359 mounting of an effective IFN $\beta$  immune response against influenza virus, possibly through  
 360 provision for fatty acyl groups for activation of IFITM3.

361



362

363 **Figure 3: FASN-dependent incorporation of Alk-4 at known myristoylation sites.** 293Ts  
364 were transfected overnight with plasmids encoding MA-Flag (MA), or the myristoylation  
365 deficient G2A-MA-Flag(G2A), and incubated for 24 hours either with Alk-4, or Alk-12. 10uM of  
366 the FASN inhibitor Fasnall was added one-hour post-transfection. **(a)** Immunoprecipitation of  
367 MA-Flag and click reaction with TAMRA azide revealed labeling of WT MA with Alk-4 and not  
368 G2A-MA, suggesting that Alk-4 labels MA at its known myristoylation site. FASN inhibition with  
369 Fasnall reduced labeling of MA by Alk-4, suggesting that FASN is required for labeling of MA  
370 by Alk-4. Alk-12 also labeled MA in both cells treated and untreated with Fasnall, indicating  
371 that Fasnall does not inhibit NMT function. **(b)** On click reaction with diazo azido biotin,  
372 streptavidin pulldown, and selective elution of Alk-4 labeled proteins, only WT-MA was labeled  
373 by Alk-4 and not G2A-MA, and Fasnall treatment also inhibited Alk-4 labeling of MA,  
374 corroborating our findings that FASN is required for labeling of MA by Alk-4 at its myristoylation  
375 site.

376

377

378

379

380

381

382

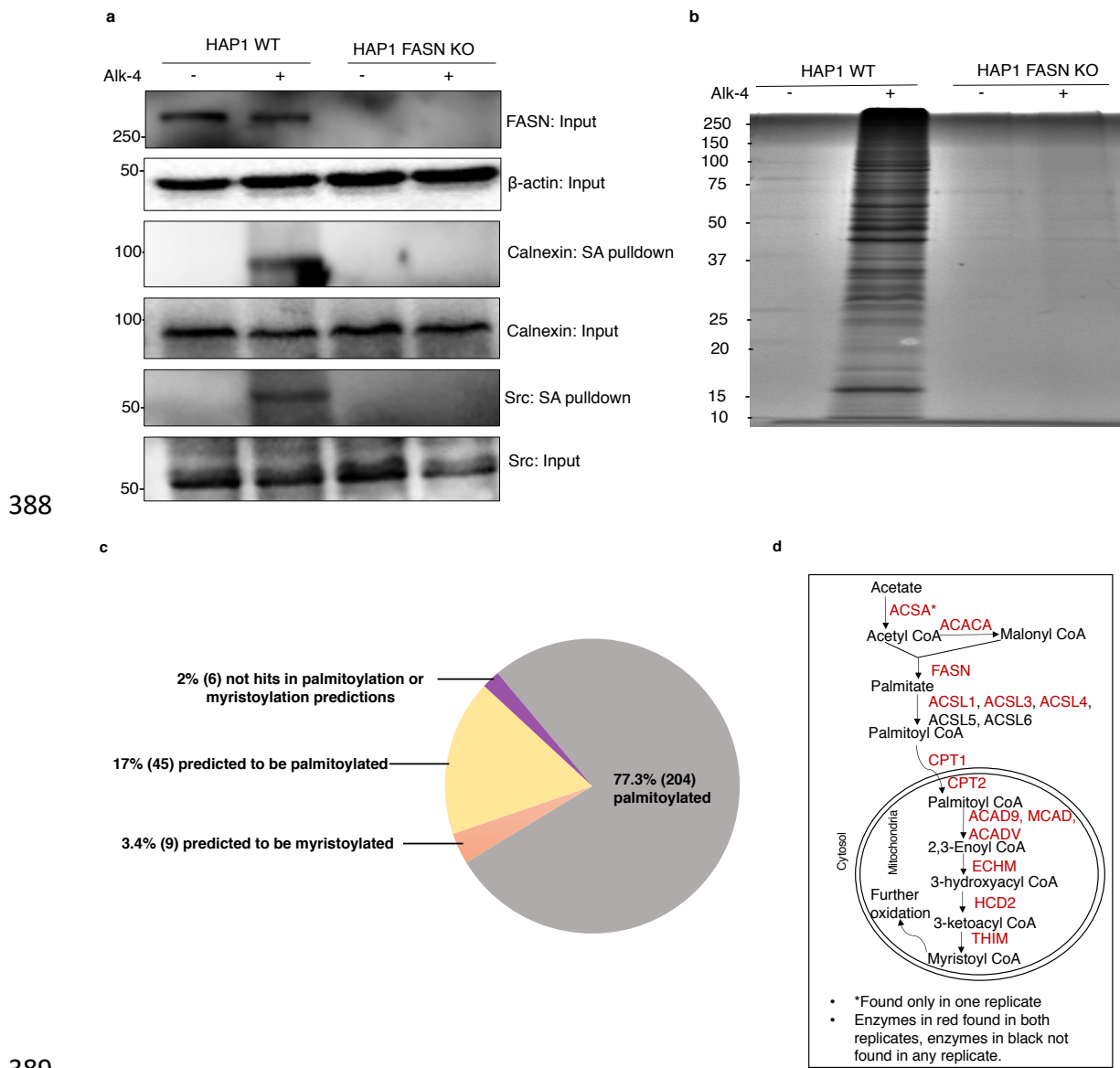
383

384

385

386

387



388

389

390 **Figure 4: FASN-dependent purification of myristoylated and palmitoylated proteins from**  
 391 **Alk-4 labeled cells.** HAP1 wild-type (WT) and HAP1 FASN knockout (KO) cells were labeled  
 392 with Alk-4, click reacted with diazo azido biotin, and labeled proteins were purified using  
 393 streptavidin beads and eluted using sodium dithionite. **(a)** Western blotting indicates that  
 394 proteins known to be palmitoylated (Calnexin) and myristoylated (Src) can be purified from  
 395 cells in an Alk-4 and FASN dependent manner. **(b)** Coomassie staining of the streptavidin (SA)  
 396 pulldown fraction revealed recovery of several proteins only in WT cells labeled with Alk-4. **(c)**  
 397 Proteomics analysis of SA pulldown fraction revealed that 77% of proteins selectively  
 398 recovered in the WT Alk-4 cells are found in at least one palmitoyl proteome or experimentally  
 399 validated to be palmitoylated based on the SwissPalm database (Dataset 3). Additionally, 17%  
 400 of proteins are predicted to be palmitoylated, based both on GPS-lipid analysis using high  
 401 confidence settings, CSS-Palm, and SwissPalm (Dataset 1). GPS-Lipid analysis also revealed  
 402 3% of proteins are predicted to be myristoylated (consensus N-terminal Glycine and non-  
 403 consensus sequence), while 2% of the proteins were not hits on prediction algorithms but had  
 404 isoforms and cysteines as per SwissPalm analysis. **(d)** Proteomics analysis of SA pulldown  
 405 fraction (n=2) revealed recovery of enzymes involved in elongation of short chain fatty acids,  
 406 as well as enzymes involved in the mitochondrial beta-oxidation pathway for oxidation of long

407 chain fatty acids. Long chain fatty acid such as palmitic acid and its oxidized product myristic  
408 acid can be used for fatty acylation of proteins.  
409  
410  
411  
412



## 413 References

- 414 1. Resh, M. D. Fatty acylation of proteins: The long and the short of it. *Prog Lipid Res* **63**,  
415 120–131 (2016).
- 416 2. Suburu, J. *et al.* Fatty acid metabolism: Implications for diet, genetic variation, and  
417 disease. *Food Bioscience* (2013). doi:10.1016/j.fbio.2013.07.003
- 418 3. Liu, H., Liu, J. Y., Wu, X. & Zhang, J. T. Biochemistry, molecular biology, and  
419 pharmacology of fatty acid synthase, an emerging therapeutic target and  
420 diagnosis/prognosis marker. *International Journal of Biochemistry and Molecular Biology*  
421 (2010).
- 422 4. Kuhajda, F. P. Fatty-acid synthase and human cancer: New perspectives on its role in  
423 tumor biology. *Nutrition* (2000). doi:10.1016/S0899-9007(99)00266-X
- 424 5. Zhang, H. *et al.* Differential regulation of host genes including hepatic fatty acid synthase  
425 in HBV-transgenic mice. *J Proteome Res* **12**, 2967–2979 (2013).
- 426 6. Tongluan, N. *et al.* Involvement of fatty acid synthase in dengue virus infection. *Virology*  
427 **14**, 28 (2017).
- 428 7. Li, Y., Webster-Cyriaque, J., Tomlinson, C. C., Yohe, M. & Kenney, S. Fatty Acid  
429 Synthase Expression Is Induced by the Epstein-Barr Virus Immediate-Early Protein  
430 BRLF1 and Is Required for Lytic Viral Gene Expression. *J. Virol.* (2004).  
431 doi:10.1128/jvi.78.8.4197-4206.2004
- 432 8. Naseri, N. *et al.* Modulation of fatty acid synthase enzyme activity and expression  
433 during hepatitis C virus replication. *Chem. Biol.* **20**, 570–82 (2013).
- 434 9. Kulkarni, M. M. *et al.* Cellular fatty acid synthase is required for late stages of HIV-1  
435 replication. *Retrovirology* **14**, 45 (2017).
- 436 10. Bakhache, W. *et al.* Fatty acid synthase and stearoyl-CoA desaturase-1 are conserved  
437 druggable cofactors of Old World Alphavirus genome replication. *Antiviral Res.* (2019).  
438 doi:10.1016/j.antiviral.2019.104642
- 439 11. Zhang, N., Zhao, H. & Zhang, L. Fatty Acid Synthase Promotes the Palmitoylation of  
440 Chikungunya Virus nsP1. *J. Virol.* (2018). doi:10.1128/jvi.01747-18
- 441 12. Krishnan, M. N. *et al.* RNA interference screen for human genes associated with West  
442 Nile virus infection. *Nature* **455**, 242–245 (2008).
- 443 13. Martín-Acebes, M. A., Blázquez, A. B., Jiménez de Oya, N., Escribano-Romero, E. &  
444 Saiz, J. C. West Nile virus replication requires fatty acid synthesis but is independent on  
445 phosphatidylinositol-4-phosphate lipids. *PLoS One* **6**, e24970 (2011).
- 446 14. Hang, H. C. & Linder, M. E. Exploring protein lipidation with chemical biology. *Chemical*  
447 *Reviews* (2011). doi:10.1021/cr2001977
- 448 15. Rodenburg, R. N. P. *et al.* Stochastic palmitoylation of accessible cysteines in  
449 membrane proteins revealed by native mass spectrometry. *Nat. Commun.* (2017).  
450 doi:10.1038/s41467-017-01461-z
- 451 16. Draper, J. M. & Smith, C. D. Palmitoyl acyltransferase assays and inhibitors (Review).  
452 *Molecular Membrane Biology* (2009). doi:10.1080/09687680802683839

- 453 17. Gao, X. & Hannoush, R. N. A Decade of Click Chemistry in Protein Palmitoylation:  
454 Impact on Discovery and New Biology. *Cell Chemical Biology* (2018).  
455 doi:10.1016/j.chembiol.2017.12.002
- 456 18. Yap, M. C. *et al.* Rapid and selective detection of fatty acylated proteins using  $\omega$ -alkynyl-  
457 fatty acids and click chemistry. *J. Lipid Res.* (2010). doi:10.1194/jlr.D002790
- 458 19. Thiele, C. *et al.* Tracing fatty acid metabolism by click chemistry. *ACS Chem Biol* **7**,  
459 2004–2011 (2012).
- 460 20. Ourailidou, M. E., Zwinderman, M. R. H. & Dekker, F. J. Bioorthogonal metabolic  
461 labelling with acyl-CoA reporters: Targeting protein acylation. *MedChemComm* (2016).  
462 doi:10.1039/c5md00446b
- 463 21. Charron, G. *et al.* Robust fluorescent detection of protein fatty-acylation with chemical  
464 reporters. *J Am Chem Soc* **131**, 4967–4975 (2009).
- 465 22. Yount, J. S. *et al.* Palmitoylome profiling reveals S-palmitoylation-dependent antiviral  
466 activity of IFITM3. *Nat Chem Biol* **6**, 610–614 (2010).
- 467 23. Chesarino, N. M. *et al.* Chemoproteomics reveals Toll-like receptor fatty acylation. *BMC*  
468 *Biol* **12**, 91 (2014).
- 469 24. Yang, Y. Y., Ascano, J. M. & Hang, H. C. Bioorthogonal chemical reporters for  
470 monitoring protein acetylation. *J Am Chem Soc* **132**, 3640–3641 (2010).
- 471 25. Mitchell, D. A., Vasudevan, A., Linder, M. E. & Deschenes, R. J. Protein palmitoylation  
472 by a family of DHHC protein S-acyltransferases. *Journal of Lipid Research* (2006).  
473 doi:10.1194/jlr.R600007-JLR200
- 474 26. Greaves, J. *et al.* Molecular basis of fatty acid selectivity in the zDHHC family of S-  
475 acyltransferases revealed by click chemistry. *Proc Natl Acad Sci U S A* **114**, E1365–  
476 E1374 (2017).
- 477 27. Jennings, B. C. & Linder, M. E. DHHC protein S-acyltransferases use similar ping-pong  
478 kinetic mechanisms but display different acyl-CoA specificities. *J Biol Chem* **287**, 7236–  
479 7245 (2012).
- 480 28. Muszbek, L., Haramura, G., Cluette-Brown, J. E., Van Cott, E. M. & Laposata, M. The  
481 pool of fatty acids covalently bound to platelet proteins by thioester linkages can be  
482 altered by exogenously supplied fatty acids. *Lipids* **34 Suppl**, S331-7 (1999).
- 483 29. Hallak, H. *et al.* Covalent binding of arachidonate to G protein alpha subunits of human  
484 platelets. *J Biol Chem* **269**, 4713–4716 (1994).
- 485 30. Veit, M., Reverey, H. & Schmidt, M. F. Cytoplasmic tail length influences fatty acid  
486 selection for acylation of viral glycoproteins. *Biochem J* **318** ( Pt 1, 163–172 (1996).
- 487 31. Thinon, E., Fernandez, J. P., Molina, H. & Hang, H. C. Selective Enrichment and Direct  
488 Analysis of Protein S-Palmitoylation Sites. *J Proteome Res* **17**, 1907–1922 (2018).
- 489 32. McMichael, T. M. *et al.* The palmitoyltransferase ZDHHC20 enhances interferon-induced  
490 transmembrane protein 3 (IFITM3) palmitoylation and antiviral activity. *J Biol Chem* **292**,  
491 21517–21526 (2017).
- 492 33. Percher, A. *et al.* Mass-tag labeling reveals site-specific and endogenous levels of

- 493 protein S-fatty acylation. *Proc Natl Acad Sci U S A* **113**, 4302–4307 (2016).
- 494 34. Farazi, T. A., Waksman, G. & Gordon, J. I. The biology and enzymology of protein N-  
495 myristoylation. *J Biol Chem* **276**, 39501–39504 (2001).
- 496 35. Alwarawrah, Y. *et al.* Fasnall, a Selective FASN Inhibitor, Shows Potent Anti-tumor  
497 Activity in the MMTV-Neu Model of HER2(+) Breast Cancer. *Cell Chem Biol* **23**, 678–688  
498 (2016).
- 499 36. Lakkaraju, A. K. K. *et al.* Palmitoylated calnexin is a key component of the ribosome-  
500 translocon complex. *EMBO J.* (2012). doi:10.1038/emboj.2012.15
- 501 37. Patwardhan, P. & Resh, M. D. Myristoylation and Membrane Binding Regulate c-Src  
502 Stability and Kinase Activity. *Mol. Cell. Biol.* (2010). doi:10.1128/mcb.00246-10
- 503 38. Resh, M. D. Myristylation and palmitoylation of Src family members: The fats of the  
504 matter. *Cell* (1994). doi:10.1016/0092-8674(94)90104-X
- 505 39. Wakil, S. J. Fatty acid synthase, a proficient multifunctional enzyme. *Biochemistry* **28**,  
506 4523–4530 (1989).
- 507 40. Xie, Y. *et al.* GPS-Lipid: A robust tool for the prediction of multiple lipid modification sites.  
508 *Sci. Rep.* (2016). doi:10.1038/srep28249
- 509 41. Ren, J. *et al.* CSS-Palm 2.0: An updated software for palmitoylation sites prediction.  
510 *Protein Eng. Des. Sel.* (2008). doi:10.1093/protein/gzn039
- 511 42. Munger, J. *et al.* Systems-level metabolic flux profiling identifies fatty acid synthesis as a  
512 target for antiviral therapy NIH Public Access Author Manuscript. *Nat Biotechnol* **26**,  
513 1179–1186 (2008).
- 514 43. Lee, M. *et al.* Fatty acid synthase inhibition prevents palmitoylation of SARS-CoV2 spike  
515 protein and improves survival of mice infected with murine hepatitis virus. Preprint at  
516 <https://www.biorxiv.org/content/10.1101/2020.12.20.423603v1> (2020).  
517 doi:10.1101/2020.12.20.423603
- 518 44. Aquino, I. G. de *et al.* Anticancer properties of the fatty acid synthase inhibitor TVB-3166  
519 on oral squamous cell carcinoma cell lines. *Arch. Oral Biol.* (2020).  
520 doi:10.1016/j.archoralbio.2020.104707
- 521 45. Zaytseva, Y. Y. *et al.* Preclinical evaluation of novel fatty acid synthase inhibitors in  
522 primary colorectal cancer cells and a patient-derived xenograft model of colorectal  
523 cancer. *Oncotarget* **9**, 24787–24800 (2018).
- 524 46. Zhang, N., Zhao, H. & Zhang, L. Fatty Acid Synthase Promotes the Palmitoylation of  
525 Chikungunya Virus nsP1. *J Virol* **93**, (2019).
- 526 47. Kim, Y.-C. *et al.* Toll-like receptor mediated inflammation requires FASN-dependent  
527 MYD88 palmitoylation. *Nat. Chem. Biol.* (2019). doi:10.1038/s41589-019-0344-0
- 528 48. Kaemmerer, E. & Gassler, N. Wnt lipidation and modifiers in intestinal carcinogenesis  
529 and cancer. *Cancers* (2016). doi:10.3390/cancers8070069
- 530 49. Lynes, E. M. *et al.* Palmitoylation is the switch that assigns calnexin to quality control or  
531 ER Ca<sup>2+</sup> signaling. *J. Cell Sci.* (2013). doi:10.1242/jcs.125856

- 532 50. Kim, S. *et al.* Blocking myristoylation of Src inhibits its kinase activity and suppresses  
533 prostate cancer progression. *Cancer Res.* (2017). doi:10.1158/0008-5472.CAN-17-0981
- 534 51. Fiorentino, M. *et al.* Overexpression of fatty acid synthase is associated with  
535 palmitoylation of Wnt1 and cytoplasmic stabilization of beta-catenin in prostate cancer.  
536 *Lab Invest* **88**, 1340–1348 (2008).
- 537 52. Yao, C. H. *et al.* Exogenous Fatty Acids Are the Preferred Source of Membrane Lipids in  
538 Proliferating Fibroblasts. *Cell Chem Biol* **23**, 483–493 (2016).
- 539 53. Chen, M. & Huang, J. The expanded role of fatty acid metabolism in cancer: new  
540 aspects and targets. *Precis. Clin. Med.* **2**, 183–191 (2019).
- 541 54. Ventura, R. *et al.* Inhibition of de novo Palmitate Synthesis by Fatty Acid Synthase  
542 Induces Apoptosis in Tumor Cells by Remodeling Cell Membranes, Inhibiting Signaling  
543 Pathways, and Reprogramming Gene Expression. *EBIOM* **2**, 808–824 (2015).
- 544 55. Zhu, Y. *et al.* Heme Oxygenase 2 Binds Myristate to Regulate Retrovirus Assembly and  
545 TLR4 Signaling. *Cell Host Microbe* (2017). doi:10.1016/j.chom.2017.01.002
- 546 56. Hach, J. C., McMichael, T., Chesarino, N. M. & Yount, J. S. Palmitoylation on Conserved  
547 and Nonconserved Cysteines of Murine IFITM1 Regulates Its Stability and Anti-Influenza  
548 A Virus Activity. *J. Virol.* **87**, 9923–9927 (2013).
- 549 57. Yount, J. S., Kraus, T. A., Horvath, C. M., Moran, T. M. & López, C. B. A Novel Role for  
550 Viral-Defective Interfering Particles in Enhancing Dendritic Cell Maturation. *J. Immunol.*  
551 (2006). doi:10.4049/jimmunol.177.7.4503
- 552 58. Moltedo, B., Li, W., Yount, J. S. & Moran, T. M. Unique type I interferon responses  
553 determine the functional fate of migratory lung dendritic cells during influenza virus  
554 infection. *PLoS Pathog.* (2011). doi:10.1371/journal.ppat.1002345
- 555 59. Merrill, C. R. Gel-staining techniques. *Methods Enzymol.* (1990). doi:10.1016/0076-  
556 6879(90)82038-4
- 557
- 558
- 559
- 560
- 561
- 562
- 563
- 564
- 565
- 566
- 567
- 568
- 569
- 570